

Computational Efficacy of Hamiltonian
Moments-based Methods for the Calculation of
Non-Tractable Potentials

A Thesis in Physics

by

Ian Lowry

Submitted in Partial Fulfillment

of the Requirements

for the Degree of

Bachelor of Arts

With Specialized Honors in Physics

May 2015

Abstract

Two versions of the connected moments expansion, those commonly known as the CMX-HW and the CMX-LT, as well as Lanczos tri-diagonalization were computed up to 7th order for the ground state and first excited state of the anharmonic oscillator with $V = x^2 + \lambda x^4$. There is no exact solution for this potential, and so it can only be approximated numerically. Trial wave functions for each method were pre-conditioned by using variational analysis. The results were compared to previously published figures, and the computation times to each other. Lanczos tri-diagonalization was found to be the most accurate and quickest method, with CMX-LT matching its accuracy but being far slower, and CMX-HW being slightly less accurate and taking similar time to CMX-LT. The first excited state for both connected moments expansions was more accurate and quicker than the ground state, however the first excited state in Lanczos tri-diagonalization had extremely poor accuracy. The preconditioning was found to improve the accuracy of the calculation by more than two orders of magnitude. Additionally, a brief study of trial wave function kurtoses was conducted, which found no systematic effect of kurtosis on the accuracy of the approximation. All calculations were carried out in Mathematica 9.0 run on a laptop computer.

Contents

1	Introduction	1
2	Theory	6
2.1	Dirac Notation	6
2.2	The t -expansion	7
2.3	Connected-Moments Expansion	9
2.4	Lanczos Tri-Diagonalization	10
3	Variational Analysis	13
4	Applications	16
4.1	The Code	16
4.1.1	Connected Moments Expansion Code	16
4.1.2	Lanczos Tri-Diagonalization Code	20
4.2	Anharmonic Oscillator	21
4.2.1	Kurtosis Effects	23
5	Results	25
5.1	Anharmonic Oscillator	25
5.1.1	Connected Moments Expansion	25

5.1.2	Kurtosis Effects	28
5.1.3	Lanczos Tri-Diagonalization	32
6	Conclusions	34
A	CMX Code	38
B	Lanczos Tri-Diagonalization Code	41
C	Further Data Tables	42

Chapter 1

Introduction

One of the greatest successes in quantum mechanics is Schrödinger's time-dependent wave equation:[1]

$$i\hbar\frac{\partial}{\partial t}\Psi(\mathbf{r}, t) = \hat{H}\Psi(\mathbf{r}, t). \quad (1.1)$$

In this equation \hat{H} is the Hamiltonian operator, \hbar is Planck's constant divided by 2π , i is the imaginary number $\sqrt{-1}$, and Ψ is the wave function of the particle. The absolute square of the wave function, $|\Psi|^2 = \Psi^*\Psi$, is the probability density of finding the particle at particular spatial and temporal coordinates, and is the best possible description of any quantum mechanical object. In principle, this equation can give the wave function of any particle under any circumstances and predict it for all time. The Hamiltonian in one dimension is given by

$$\hat{H} = -\frac{\hbar^2}{2m}\frac{\partial^2}{\partial x^2} + V(x). \quad (1.2)$$

Where $V(x)$ is the potential function for this particle. Typically Ψ is taken to be separable into a spatial part and a temporal part:

$$\Psi(x, t) = \psi(x)T(t). \quad (1.3)$$

Substituting both of these into Eq. 1.1 and moving the time functions to the left hand side and the spatial functions to the right gives:

$$\frac{i\hbar}{T(t)} \frac{\partial}{\partial t} T(t) = -\frac{\hbar^2}{2m\psi(x)} \frac{\partial^2}{\partial x^2} \psi(x) + V(x). \quad (1.4)$$

Since the left hand side of this equation depends only on the time and the right hand side only on the position they must both be equal to some constant, which we call E . The left hand side can then be readily solved without further information, giving:

$$T(t) = e^{-iEt/\hbar}. \quad (1.5)$$

The solution to the right hand side depends on $V(x)$, and this equation is so important that it has its own name, the time independent Schrödinger equation, and is even sometimes referred to simply as the Schrödinger equation,

$$-\frac{\hbar^2}{2m} \frac{d^2}{dx^2} \psi(x) + V(x)\psi(x) = E\psi(x). \quad (1.6)$$

The solutions of this equation will then be the stationary states of the system, and E will be the energy of the state.

These equations can give the exact wave function Ψ of any particle under any circumstances. However, they are differential equations, and it is quite common for differential equations to be difficult or even impossible to solve exactly by known methods. In the case of the Schrodinger Equation, it is possible to find analytic solutions in just a few simple cases: the "particle in a box" problem, with a potential which is zero in some range and infinite elsewhere; the harmonic oscillator, with a potential of the form Ax^2 ; and the Hydrogen atom, which is solved in spherical coordinates with a potential of the form $-A/r$. For all other cases that proves to be impossible. Instead, the best we can do is to create a

numerical approximation to what the solutions of that wave function should be.

These approximations are typically very difficult to find to high accuracy. One commonly used scheme is that arising out of perturbation theory, which treats the system as similar to one of those simple ones which can be solved but with a small additional term in the potential, the perturbation,

$$H = H^0 + H'. \quad (1.7)$$

To first order, the energy approximation will then be the energy of the solved system in a particular state plus the expectation value of the perturbation term in that state, which is equivalent to the expectation value of the full perturbed Hamiltonian in that state[1]

$$E_n^0 + E_n^1 = \int_{-\infty}^{\infty} \psi_n^{0*} H^0 \psi_n^0 dx + \int_{-\infty}^{\infty} \psi_n^{0*} H' \psi_n^0 dx. \quad (1.8)$$

This is also the first order of the methods used in this thesis, which will be seen to be not very accurate.

The second order correction is not nearly so simple. It is given by,

$$E_n^2 = \sum_{m \neq n} \frac{\left(\int_{-\infty}^{\infty} \psi_m^{0*} H' \psi_n^0 \right)^2}{E_n^0 - E_m^0} \quad (1.9)$$

where ψ_n^0 is the n th energy state of the solved system, E_n^0 is the corresponding energy, and H' is the perturbation.[1] The problem with this method should now be obvious: it requires the computation of a complicated infinite sum to provide even the second order correction, so that unless we are very lucky and have a perturbation which gives a simple sum it may be impossible to calculate that term exactly. The higher order terms are even worse, and so, unless the perturbation is very small so that the first order approximation is very accurate, this method tends to have limited usefulness.

Fortunately, this is not the only option. Many other approximation techniques can be devised. Martin, Castro, and Paz used one of these, which they described as a multi-point quasi-rational approximation, to produce a full 11 decimal places of accuracy for the system they were looking at.[2] Here again, however, we run into calculation problems. Merely defining their method requires dozens of equations, and some of them include infinite sums, although much simpler ones. The worst part, though, is the fact that, in setting up the method, they had to calculate approximate solutions to a series of differential equations by using the shooting method. This method approximates the solution to a differential equation whose value at some point is known by solving the equation with a series of initial values and then using the solution which provides the closest match to the known value. Of course, frequently the initial value problems can only be approximated, and so just this set up portion will require a great deal of computational effort, before even reaching the primary calculation. Further, the entire method was derived assuming the potential to have the form $x^a + \lambda x^b$, where a , b , and λ are constants, and so cannot be used for any other case.

There are alternatives. Techniques which, while less accurate, are much shorter and easier to calculate. “Less accurate” and “easier to calculate” are disturbingly qualitative terms, and so the primary goal of this project was to examine three of those techniques and determine how accurate they are to those longer methods, and how much time is required to compute their results with Mathematica 9 run on a personal computer.

The techniques selected for inclusion were two variants on what is known as the Connected Moments Expansion, which are referred to throughout the literature as the CMX-HW and the CMX-LT,[3] along with Lanczos Tri-Diagonalization.[4] All three methods can also readily generate excited state energies, and so the first two excited states were also calculated.

Additionally, a relatively novel refinement was added to all three. Each uses a trial wave

function and converges to the true energy of the system as the order of the approximation increases. That allows for easy hybridization of these methods with the variational analysis scheme. This is a well established method which takes a trial wave function, modifies it with a parameter, and then sets the parameter so that the expectation value of the Hamiltonian is a minimum. This is then a better approximation to the true wave function and energy than the original trial wave function. For this project, that improved wave function was then fed into the methods listed above, improving their accuracy.

Chapter 2

Theory

In this chapter we will describe each method used in detail, along with some of the theory and history underlying them.

2.1 Dirac Notation

Before we begin, it will be convenient to introduce Dirac's bra-ket notation. To motivate it, note that the expectation value of any property in quantum mechanics, $\langle O \rangle$, is given by

$$\langle O \rangle = \int_{-\infty}^{\infty} \psi^*(x) \hat{O} \psi(x) dx. \quad (2.1)$$

As is always the case in quantum mechanics, ψ^* is the complex conjugate of ψ , and \hat{O} is the operator associated with the quantity O . We have already seen one such operator, the Hamiltonian given by Eq. 1.2, which is associated with the energy of the system. There is such an operator for position, momentum, spin in any direction, and any other desired quantity. Thus, equations of the same form as Eq. 2.1 are extremely common, and so it is useful to have a shorthand for them.

In bra-ket notation, that equation can be written as

$$\langle O \rangle = \langle \psi | \hat{O} | \psi \rangle. \quad (2.2)$$

The bra $\langle \psi |$ indicates that ψ^* should be used, the ket $|\psi\rangle$ that ψ should be used, $\hat{O}|\psi\rangle$ that \hat{O} should act on ψ , and the whole combination that an integral over all space should be taken. This notation has a further advantage beyond just being short, however.

We have already discussed the Hamiltonian $H|\psi\rangle = \hat{H}(\psi)$. What we have not mentioned is that terms such as $\hat{H}(\hat{H}(\psi))$ will become essential to this project. In Dirac notation we can write this conveniently as $H^2|\psi\rangle$, and we can write similarly that $\hat{H}(\hat{H}(\hat{H}(\psi))) = H^3|\psi\rangle$, and, crucially, the general form $H^n|\psi\rangle$. The expectation value of this general form, $\langle \psi | H^n | \psi \rangle$, and variations on it, will appear in all three of the methods included, and is referred to as a Hamiltonian moment.

2.2 The t -expansion

The precursor to the Connected Moments Expansions we will use was the t -expansion, which was first derived in a 1984 paper by Horn and Weinstein.[5] This is intended for potentials which can't be solved analytically, and uses the true Hamiltonian together with a guess at the wave function, which must not be orthogonal to the true ground state wave function. They began with the statement that the following equation will converge to the true ground state energy as t approaches infinity

$$E(t) = \frac{\langle \psi_0 | \hat{H} e^{-t\hat{H}} | \psi_0 \rangle}{\langle \psi_0 | e^{-t\hat{H}} | \psi_0 \rangle}. \quad (2.3)$$

Here ψ_0 is the guess wave function. From this they expanded the exponentials in their Taylor series

$$e^x = 1 + x + \frac{x^2}{2!} + \frac{x^3}{3!} \cdots = \sum_{n=0}^{\infty} \frac{x^n}{n!}. \quad (2.4)$$

By matching powers of t in this expansion they derived the infinite sum

$$E(t) = \sum_{n=0}^{\infty} \frac{(-t)^n}{n!} I_{n+1} \quad (2.5)$$

where

$$I_n = \langle H^n \rangle - \sum_{k=0}^{n-2} \binom{n-1}{k} I_{k+1} \langle H^{n-k-1} \rangle \quad (2.6)$$

$$\text{and } \langle H^n \rangle = \langle \psi | H^n | \psi \rangle. \quad (2.7)$$

This uses the choose function given by

$$\binom{n}{p} = \frac{n!}{p!(n-p)!}. \quad (2.8)$$

Explicitly, the first three connected moments are,

$$I_1 = \langle H \rangle - 0, \quad (2.9)$$

$$I_2 = \langle H^2 \rangle - \langle H \rangle \langle H \rangle, \text{ and} \quad (2.10)$$

$$I_3 = \langle H^3 \rangle - \langle H \rangle \langle H^2 \rangle - 3(\langle H^2 \rangle - \langle H \rangle^2) \langle H \rangle. \quad (2.11)$$

From these equations they were able to construct approximations to the true energy of two complex systems, and found that these approximations were significantly improved over previously published approximations.

2.3 Connected-Moments Expansion

In 1987 Cioslowski created a new approximation based on Horn and Weinstein's.[6] His approximation, like theirs, relies on the connected moments given by Eq. 2.6. He expanded Eq. 2.5 as a sum of decaying exponentials,

$$\sum_{n=0}^{\infty} \frac{(-t)^n}{n!} I_{n+1} = \sum_{j=0}^{\infty} A_j e^{-b_j t}, \quad (2.12)$$

and was able to match coefficients to eliminate t and give an infinite sum of just the I_n 's,

$$E_0 = I_1 - \frac{I_2^2}{I_3} - \left(\frac{1}{I_3} \right) \frac{(I_4 I_2 - I_3^2)^2}{I_5 I_3 - I_4^2} - \dots \quad (2.13)$$

Deriving further terms in this expansion is no easier than it appears, and so we will rely on the general form used by Witte for the series up to the n th term,[3]

$$S_{1,n} = I_n \quad (2.14)$$

$$S_{m,n} = S_{m-1,n} S_{m-1,n+2} - S_{m-1,n+1}^2 \quad (2.15)$$

$$E_0 = I_1 - \sum_{m=1}^n \frac{S_{m,2}^2}{\prod_{k=1}^m S_{k,3}} \quad (2.16)$$

Remarkably, this is not the only approximation based on the connected moments which is valid. Witte mentions four of these: the CMX-HW, which we have been discussing; the CMX-SD; the CMX-LT; and the AMX.[3] Mancini et al. published a further variation in 2005 which they named the Generalized Moments Expansion, or GMX, which uses a pair of parameters in the S functions, Eqs. 2.14 and 2.15, to include the CMX-HW, AMX, and many other unnamed expansions.[7] They did, however, find that using low values of those parameters tended to produce better results, with the CMX-HW, followed by the AMX, being the two lowest valued expansions.

For this thesis we will use the CMX-HW and the CMX-LT expansions. The CMX-LT is not included within the GMX, and has a very different appearance: it is based on matrix multiplication, with the size of the matrices being one less than the order of the expansion. Two of the earliest derivations of this expansion were published by Knowles.[8] It is given by the following simple equation[3]

$$E_0 = I_1 - \begin{pmatrix} I_2 & I_3 & \dots & I_n \end{pmatrix} \begin{pmatrix} I_3 & I_4 & \dots & I_{n+1} \\ I_4 & I_5 & \dots & I_{n+2} \\ \vdots & \vdots & \ddots & \vdots \\ I_{n+1} & I_{n+2} & \dots & I_{2n-1} \end{pmatrix}^{-1} \begin{pmatrix} I_2 \\ I_3 \\ \vdots \\ I_n \end{pmatrix}. \quad (2.17)$$

Connected moments expansions have one further advantage: they can be readily used to calculate the energies of excited states as well as the ground state. The connected moments require a trial wave function which is not orthogonal to the true wave function. Should the trial wave function be more closely related to the true wave function of the first excited state than of the ground state the expansion will converge to the first excited state. The same is true for any excited state. This stands in stark contrast to many other methods which either cannot produce the excited states at all or else require a great deal of work to do so.

2.4 Lanczos Tri-Diagonalization

The third approximation technique used here is Lanczos tri-diagonalization. This method is commonly used to find approximations to the eigenvalues of very large matrices, but is equally applicable to eigenvalues of differential equations. Using the initial matrix or equation, together with a trial vector or function, it generates a simplified matrix with non-zero elements only along the main diagonal and adjacent to it. Because it has these three diago-

nal lines of non-zero elements, this is referred to as a tri-diagonal matrix. The eigenvalues of this new matrix will be approximately equal to the eigenvalues of the original matrix or equation, and will be much easier to calculate since the zeroes eliminate so many terms of the calculation. It should be noted that this will produce multiple eigenvalues simultaneously, specifically, the first n eigenvalues when the final matrix is $n \times n$, and so when using this process to find the energy of a quantum mechanical system it will automatically provide approximations to the n lowest energy states.

The algorithm is as follows[9]:

Let ψ be a starting vector and then define the following:

$$v_1 = \psi$$

$$v_0 = 0$$

$$\beta_1 = 0$$

with,

$$w_j = Av_j$$

$$\alpha_j = w_j \cdot v_j$$

$$u_j = w_j - \alpha_j v_j - \beta_j v_{j-1}$$

$$\beta_{j+1} = \|v_j\|$$

$$v_{j+1} = u_j / \beta_{j+1}$$

and from these form the matrix

$$\begin{pmatrix} \alpha_1 & \beta_2 & 0 & \cdots & 0 \\ \beta_2 & \alpha_2 & \beta_3 & & \vdots \\ 0 & \beta_3 & \alpha_3 & \ddots & 0 \\ \vdots & & \ddots & \ddots & \beta_n \\ 0 & \cdots & 0 & \beta_n & \alpha_n \end{pmatrix}. \quad (2.18)$$

To use this to find energy, we make the usual identifications of A as the Hamiltonian operator, ψ as the trial wave function, Hv_j as $H(v_j)$, $w_j \cdot v_j$ as $\langle w_j | v_j \rangle$, and $\|v_j\|$ as $\sqrt{\langle v_j | v_j \rangle}$.

With these identifications, the algorithm functions identically for matrices as it does for operators.

Chapter 3

Variational Analysis

This chapter describes the primary innovation made in this work.

As an independent technique, variational analysis takes a trial wave function $\psi_0(x)$, and modifies it by inserting a parameter to give $\psi(x, a)$. Then the parameter is set so as to minimize the expectation value of the energy in this state by expressing it as a function of the parameter, taking the derivative of the resulting function with respect to the parameter, and finding the critical points, that is, finding a such that

$$\frac{d}{da} \langle \psi(x, a) | \hat{H} | \psi(x, a) \rangle = 0. \quad (3.1)$$

The result will then be a much better estimate of the true energy and wave function.[1]

This alone provides a simple way to obtain decent estimates of the energy. However, it could also be used to precondition the trial wave function for any other method which relies on one. That is a simple matter of performing the variational analysis, and then taking the improved wave function and inputting it as the trial wave function for the other method. Since all three methods we will use begin with a trial wave function, they can all be improved with this preconditioning. This thesis is the first work to apply that preconditioning

to a Connected Moments Expansion for the anharmonic oscillator to obtain the ground state and first excited state energies.

Table 3.1 shows the results of this procedure for CMX-HW. Using CMX-HW alone, we see that the percent difference ranges between 135% and 49%, but the preconditioning reduces the difference to between 1.4% and 0.05%, an improvement of almost two orders of magnitude on the high end and almost three on the low end. This is far greater than the effects of the simple method of increasing accuracy for these expansions: simply increasing the order of the expansion, as we see that increasing the order from 1 to 7 provides a less than one order of magnitude improvement without the preconditioning, and less than two orders of magnitude with preconditioning. Naturally, combining the two produces the best results.

Table 3.1: Ground state energies and percent differences for the anharmonic oscillator using the Gaussian Eq 4.2 in CMX-HW with and without variational analysis.

λ	Martin, Castro, and Paz	Order	with V.A.		Without V.A.	
			Energy	% difference	Energy	% difference
5	2.0183406575	1	2.04704	1.422	4.75	135.342
		2	2.02303	0.232	3.58495	77.619
		3	2.02009	0.087	3.16409	56.767
		4	2.01956	0.060	3.02836	50.042
		5	2.01944	0.054	3.0013	48.701
		6	2.01942	0.053	2.99793	48.534
		7	2.01942	0.053	2.99791	48.533

Table 3.2 is the same comparison but with CMX-LT this time. The high end improvement is again from 135% to 1.4%, but the low end improvement is even greater than it was before, from 30% to 0.02%, which is more than three orders of magnitude.

Table 3.3 is this comparison again but now for Lanczos Tri-Diagonalization. We see throughout that the results are identical to those from CMX-LT, only with the first order removed. Thus the improvement is the same massive two to three orders of magnitude for conducting this simple procedure.

Table 3.2: Ground state energies and percent differences for the anharmonic oscillator using the Gaussian Eq. 4.2 in CMX-LT with and without variational analysis.

λ	Martin, Castro, and Paz	Order	with V.A.		Without V.A.	
			Energy	% difference	Energy	% difference
5	2.0183406575	1	2.04704	1.422	4.75	135.342
		2	2.02303	0.232	3.58495	77.619
		3	2.02009	0.087	3.16409	56.767
		4	2.01934	0.050	2.94032	45.680
		5	2.01904	0.035	2.79908	38.682
		6	2.01888	0.027	2.70075	33.810
		7	2.01876	0.021	2.62777	30.195

Table 3.3: Ground state energies and percent differences for the anharmonic oscillator using the Gaussian Eq. 4.2 in Lanczos Tri-Diagonalization with and without variational analysis.

λ	Martin, Castro, and Paz	Order	with V.A.		Without V.A.	
			Energy	% difference	Energy	% difference
5	2.0183406575	2	2.02305	0.233	3.59531	78.132
		3	2.02009	0.087	3.17653	57.383
		4	2.01934	0.050	2.95339	46.328
		5	2.01904	0.035	2.81226	39.335
		6	2.01888	0.027	2.71382	34.458
		7	2.01876	0.021	2.64064	30.832

Since this preconditioning is so highly effective it will be used in all other calculations in this thesis.

Chapter 4

Applications

All calculations were performed in Mathematica 9.0 running on a 2014 Dell Alienware 14 laptop with 8 GB of DDR3 RAM and a 2.5 GHz dual core Intel Core i5-4200M processor. In all cases it was found that Mathematica would crash if asked to perform very long calculations, roughly those in excess of 2.5 hours. All calculation times given were obtained using Mathematica's internal Timing function and averaged over three runs.

4.1 The Code

The basic code used for all calculations performed here is listed in the Appendices for quick copying and use. This section will go over it line by line to clarify its use.

4.1.1 Connected Moments Expansion Code

We begin with the code in Appendix A. The functions and potentials throughout are those for a Gaussian wave function and the Anharmonic Oscillator. The first two lines of this code simply check the normalization of the proposed wave function.

```
\[Psi]1[x_, a_] := ((a/Pi)^0.25) Exp[-(a*(x^2))/2]
```


The next section solves for the critical points of the Hamiltonian, with the final a values given as functions of b. Either input the result of the previous section directly and set it equal to 0, or else simplify it somewhat first, as has been done here to give a simple cubic polynomial.

```
Solve[ a^3 - a - 3 b == 0, a]
```

Typically that will generate only one real and positive result, and so that result should be used in the next section.

```
aa[b_] := (2/3)^(1/3)/
(27 b + Sqrt[3] Sqrt[-4 + 243 b^2])^(1/3)
+ (27 b + Sqrt[3] Sqrt[-4 + 243 b^2])^(1/3)/
(2^(1/3) 3^(2/3))
```

aa will then serve as the parameter function for the rest of the code.

The next line simply sets bb, the lambda value currently of interest, which is entered after the equal sign.

```
bb =;
```

And now we embark on the Connected Moments Expansions proper. The first three lines will be quite familiar: Ψ is the same one generated in the first section, V has not changed, and H is simply the Hamiltonian with constants set to 1, much like EE and FF.

```
\[Psi][x_] := ((aa[bb]/Pi)^(0.25)) Exp[-(aa[bb]*(x^2))/2]
```

```
V[x_] := x^2 + (bb)*x^4
```

```
H[f_] := Simplify[((-1) Laplacian[f, {x}] + V[x] f)]
```

```
AA[n_] :=
```

```
Integrate[\[Psi][x]*
```

```
Nest[H, \[Psi][x], n], {x, -\[Infinity], \[Infinity]}]
```

```

J[1] := J[1] =
  Integrate[\[Psi][x]*H[\[Psi][x]],
    {x, -\[Infinity], \[Infinity]}}
J[n_] := J[n] =
  AA[n] - Sum[(Binomial[n - 1, k])*(J[k + 1])*AA[n - k - 1],
    {k, 0, n - 2}]
S[1, n_] := S[1, n] = J[n]
S[m_, n_] :=
  S[m, n] = (S[m - 1, n]*S[m - 1, n + 2])
  - (S[m - 1, n + 1])^2
HW[n_] :=
  J[1] - Sum[((S[m, 2])^2)/(Product[(S[k, 3]), {k, 1, m}]),
    {m, 1, n - 1}]
LT[n_] :=
  J[1] - Det[(MatrixForm[Table[J[j], {i, 1}, {j, 2, n}]]]).
  (Inverse[MatrixForm[
    Table[J[1 + i + j], {i, n - 1}, {j, n - 1}]]]).
  (MatrixForm[Table[J[i], {i, 2, n}, {j, 1}]])]

```

AA[n_], is new. This gives the Hamiltonian moments $\langle \psi | H^n | \psi \rangle$. J[1] is the expectation value of the Hamiltonian, which is also I_1 . J[n_] is I_n , Eq. 2.6, using AA[n_] to generate all needed moments. Note that here we have used J[n_]:=J[n]=... This is not redundant, but rather informs Mathematica that it should store numerical values for this function in memory rather than recalculating them. Since this reduces calculation time by as much as half it will be used heavily. Using Simplify in the Hamiltonian is similarly unnecessary, but also greatly speeds lengthy calculations, although it does slow down short ones. S[1,n_]

and $S[m_.,n_]$ are exactly Eqs. 2.14 and 2.15, and $HW[n_]$ is the final CMX-HW expression, Eq. 2.16, to n th order. Similarly, $LT[n_]$ is Eq. 2.17 to n th order.

Extracting a final result from the code, once it has all been run, is then a simple matter of entering the desired approximation and order and then running it, for example,

```
LT[4]
```

Alternatively, if the calculation time is desired, then that command should be placed inside the timing function, for example,

```
Timing [HW[3]]
```

4.1.2 Lanczos Tri-Diagonalization Code

The code for the Lanczos Tri-Diagonalization method is in Appendix B. It is intended to be added to the end of the Appendix I code, and so it does not separately define the Hamiltonian or the parameter. The code for this approximation is then

```
\[Beta][1] = 0;
v[0] = 0;
v[1] := ((aa[bb]/Pi)^(0.25)) Exp[-(aa[bb]*(x^2))/2]
w[j_] := H[v[j]]
u[j_] := w[j] - \[Alpha][j]*v[j] - \[Beta][j]*v[j - 1]
\[Beta][j_] := \[Beta][j] = (Integrate[
    u[j - 1]*u[j - 1], {x, -\[Infinity], \[Infinity]}])^0.5
\[Alpha][j_] := \[Alpha][j] =
    (Integrate[ w[j]*v[j], {x, -\[Infinity], \[Infinity]}])
v[j_] := u[j - 1]/\[Beta][j]
```

This code matches Eqs. 2.18 almost exactly. Even the names of the functions are the same. The only differences arise from the need to make the integrations explicit, the fact that Mathematica designates functions as $f[x]$ rather than f_x , and the desire to make the program store certain results in memory, but those are little more than typesetting. The tri-diagonal $n \times n$ matrix is then given by

```
T[n_] := MatrixForm[
  Table[Piecewise[{{\[Alpha][i], j - i == 0},
    {\[Beta][i], i - j == 1}, {\[Beta][j], j - i == 1}}, 0],
    {i, n}, {j, n}]]
```

and the energies will be given by, for example

```
Eigenvalues[T[4]]
```

This will produce a list of n eigenvalues, of which the smallest will be the ground state energy, the next smallest the first excited state energy, and so on. The computation can be timed exactly as above,

```
Timing[Eigenvalues[T[2]]]
```

4.2 Anharmonic Oscillator

The primary problem discussed here is the anharmonic oscillator, for which the potential is

$$V(x) = x^2 + \lambda x^4 \quad (4.1)$$

where λ is some constant. Martin, Castro, and Paz [2] calculated energies for the ground state and the first two excited states in this problem, with λ equalling 0.5, 1, 2, 5, and 20, to 11 decimal places, and so all percent difference comparisons are to their values.

Martin et al. selected this potential primarily because it serves as a straightforward test case. That reasoning certainly applies equally well to this project, with the addition that there are now highly accurate numerical values for the energies. However, this potential also has physical significance. For example, the Higgs potential, related to the famous Higgs boson, has essentially this form, albeit with additional constants and a different variable.[10]

Since the anharmonic oscillator is similar to the harmonic oscillator, the trial wave functions were the exact solutions to the harmonic oscillator problem for the 3 lowest states, which, normalized and including the parameter, are[11]

$$\psi_0(x) = \left(\frac{a_0(\lambda)}{\pi} \right)^{0.25} e^{-\frac{a_0(\lambda)x^2}{2}}, \quad (4.2)$$

$$\psi_1(x) = \sqrt{\frac{2(a_1(\lambda))^3}{\sqrt{\pi}}} x e^{-\frac{a_1(\lambda)x^2}{2}}, \text{ and} \quad (4.3)$$

$$\psi_2(x) = (4\pi a_2(\lambda))^{0.25} (1 - 2a_2(\lambda)x^2) e^{-\frac{a_2(\lambda)x^2}{2}}. \quad (4.4)$$

with the $a_n(\lambda)$ functions being given by the minimization procedure as the solutions of, respectively,

$$a_0^3 - a_0 - 3\lambda = 0, \quad (4.5)$$

$$1.5a_1^3 - 1.5a_1 - 7.5\lambda = 0, \text{ and} \quad (4.6)$$

$$2.5a_2^3 - 2.5a_2 - 19.5\lambda = 0. \quad (4.7)$$

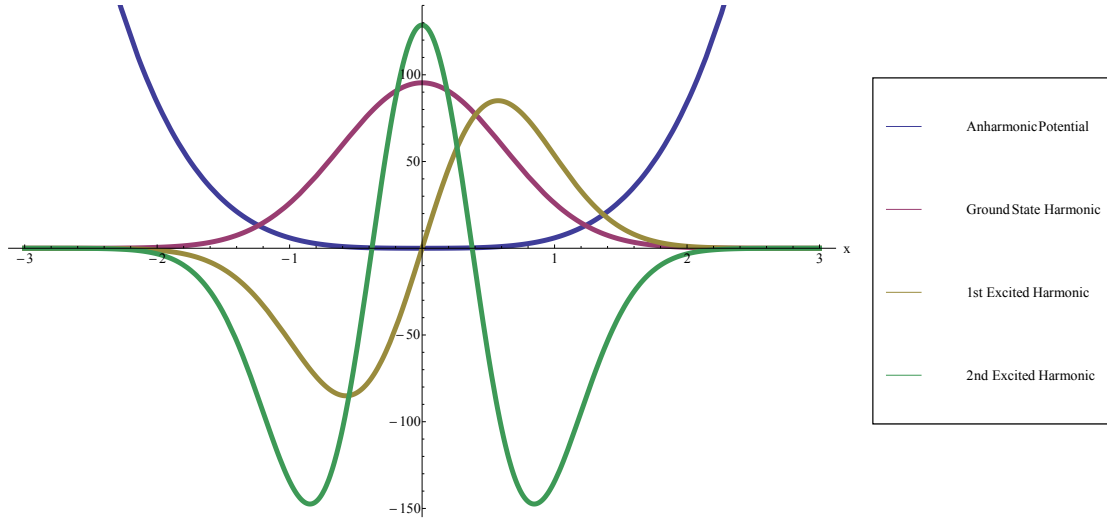


Figure 4.1: Graph of the anharmonic potential with the ground state and first two excited state wave functions for the harmonic oscillator. $\lambda = 5$

which are surprisingly simple equations. These wave functions can be seen overlaid on the potential in Figure 4.1

4.2.1 Kurtosis Effects

This study also checked whether the kurtosis of the trial wave function has any systematic effect on the rate of convergence of the series. Kurtosis is a measure of how strongly peaked a function is. One formula giving it a numerical value, sometimes referred to as the excess kurtosis, is [12]

$$K(f(x)) = \frac{\mu_4}{\mu_2^2} - 3 = \frac{\int_{-\infty}^{\infty} \left(x - \int_{-\infty}^{\infty} x f(x) dx \right)^4 f(x) dx}{\left(\int_{-\infty}^{\infty} \left(x - \int_{-\infty}^{\infty} x f(x) dx \right)^2 f(x) dx \right)^2} - 3 \quad (4.8)$$

Since the first wave function was a Gaussian, one function with higher kurtosis and one with lower kurtosis were selected. For higher kurtosis the hyperbolic secant function

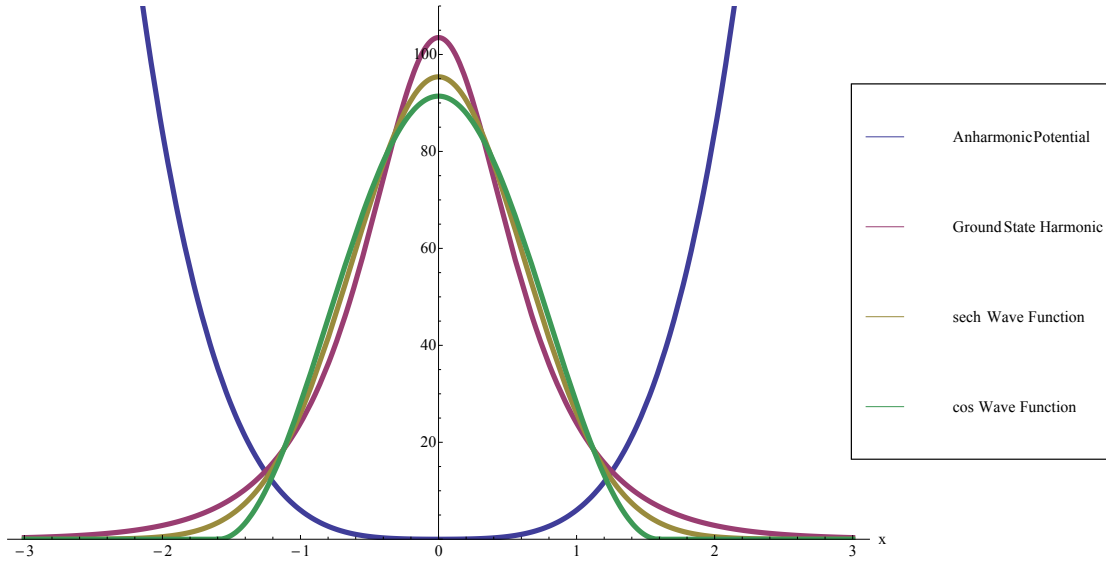


Figure 4.2: Graph of the anharmonic potential with the ground state harmonic oscillator, hyperbolic secant, and cosine wave functions. $\lambda = 5$

$$\psi_0(x) = \sqrt{\frac{a(\lambda)}{2}} \operatorname{sech}(a(\lambda)x) \quad (4.9)$$

was selected, while a single lobe of a cosine function was selected for the lower kurtosis function, given by

$$\psi_0(x) = \frac{1}{\sqrt{3a(\lambda)}} \left(1 + \cos\left(\frac{\pi}{a(\lambda)}x\right) \right) \quad (4.10)$$

which required the integration limits throughout to be changed to $-a(\lambda)$ and $a(\lambda)$, instead of $\pm\infty$. The simplicity of these limits was the reason for the choice to place the parameter in the denominator for the cosine-based wave function when it is in the numerator for all others. These can be seen in Figure 4.2 The $a(\lambda)$ functions of course had to be recalculated for each function.

Chapter 5

Results

5.1 Anharmonic Oscillator

5.1.1 Connected Moments Expansion

For the ground state accuracy ranged from 1.75% to 0.0021% difference from the Martin, Castro, and Paz results. There is minimal difference in calculation time between the CMX-HW and CMX-LT methods, however the CMX-LT is more accurate. A full listing of the energy results can be found in Tables C.1 and 5.1. To further prove the stability of the method third order CMX-HW was run for λ 's ranging from 0.1 to 6 in steps of 0.1. Any sudden jumps in these values would indicate a serious flaw in the method, as they would clearly be non-physical. The results are displayed in Figure 5.1, and can be seen to be nicely continuous. Graphs of energy vs. order are also included as Figures C.1 and 5.2. Finally, the time results for $\lambda = 2$ can be found in Tables C.2 and 5.2.

Results improved significantly for the first excited state, and the calculation time dropped. For the second excited state, however, the results were very poor, with the percent difference never dropping below 125%. These results can be seen in Tables C.3 and 5.3, and C.5

Table 5.1: Ground state energies and percent differences for the anharmonic oscillator using the gaussian Eq. 4.2 in CMX-LT.

λ	Martin, Castro, and Paz	Order	CMX-LT Energy	% difference
0.5	1.24185404314	1	1.24803	0.4973
		2	1.24239	0.0432
		3	1.24201	0.0126
		4	1.24194	0.0069
		5	1.24191	0.0045
		6	1.24189	0.0029
		7	1.24188	0.0021
1	1.3923515801	1	1.39363	0.0918
		2	1.39363	0.0918
		3	1.39276	0.0293
		4	1.39258	0.0164
		5	1.39251	0.0114
		6	1.39247	0.0085
		7	1.39244	0.0064
2	1.6075413481	1	1.625	1.0860
		2	1.61	0.1529
		3	1.6084	0.0534
		4	1.60802	0.0298
		5	1.60788	0.0211
		6	1.60779	0.0155
		7	1.60774	0.0124
5	2.0183406575	1	2.04704	1.4219
		2	2.02303	0.2323
		3	2.02009	0.0867
		4	2.01934	0.0495
		5	2.01904	0.0346
		6	2.01888	0.0267
		7	2.01876	0.0208
20	3.0099449478	1	3.0625	1.746
		2	3.0195	0.3174
		3	3.01367	0.1238
		4	3.01212	0.0723
		5	3.01148	0.0510
		6	3.01112	0.0390
		7	3.01089	0.0314

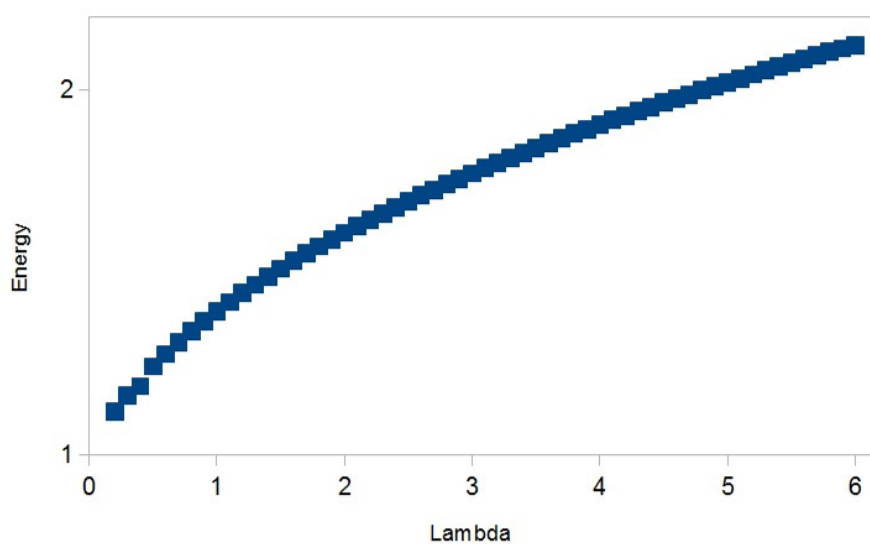


Figure 5.1: Graph of ground state energy vs. λ for 3rd order CMX-HW from $\lambda = 0.1$ to $\lambda = 6$ at intervals of 0.1

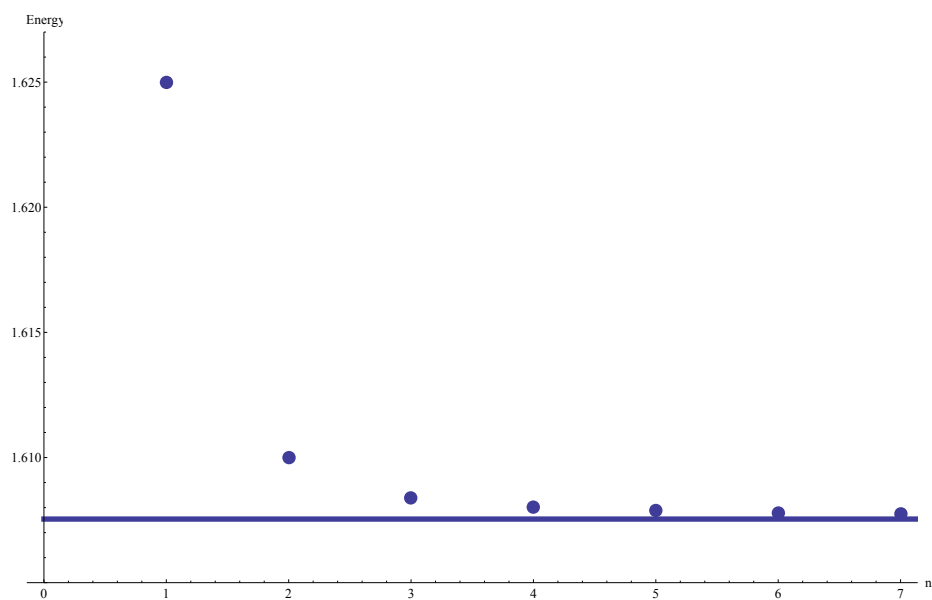


Figure 5.2: Graph of energy approximation vs. order for CMX-LT, with comparison to the Martin, Castro, and Paz result, for $\lambda = 2$.

Table 5.2: Ground state energies, percent differences, and calculation times for the anharmonic oscillator using the gaussian Eq. 4.2 in CMX-LT.

λ	Martin, Castro, and Paz	Order	CMX-LT		
			Energy	% difference	Time (s)
2	1.6075413481	1	1.625	1.0860	4.7 ± 0.8
		2	1.61	0.1529	12.9 ± 2.3
		3	1.6084	0.0534	20.8 ± 4.8
		4	1.60802	0.0298	35.8 ± 7.4
		5	1.60788	0.0211	55.1 ± 2.8
		6	1.60779	0.0155	64.5 ± 8.0
		7	1.60774	0.0124	78.3 ± 0.5

and C.7, with the energy results in Tables C.4 and 5.4 and C.6 and C.8, respectively.

5.1.2 Kurtosis Effects

Both the hyperbolic secant- and cosine-based wave functions produce much poorer results than the Gaussian one. The hyperbolic secant function, Eq. 4.9, requires the longest to calculate at first order of any of the approximations listed here, so long that even the second order cannot be calculated directly for timing, and can only be calculated by storing the first order results first. Thus only the first order times were extracted, and proved to be 106.3 ± 0.9 seconds for CMX-HW and 104.6 ± 1.4 seconds for CMX-LT. The cosine function, Eq. 4.10, does produce significantly better energy results than the secant function, however it exhibits oscillations around the true energy as the order increases, instead of a simple monotonic decrease toward it. These results can be seen in Tables C.9 and 5.5, and C.10 and 5.6, with timing results for the cosine function in Tables C.11 and 5.7, respectively.

Table 5.3: First excited state energies and percent differences for the anharmonic oscillator using the the harmonic oscillator first excited state Eq. 4.3 in CMX-LT.

λ	Martin, Castro, and Paz	Order	CMX-LT Energy	% difference
0.5	4.0519323386	1	4.06992	0.4439
		2	4.05321	0.0315
		3	4.05227	0.0083
		4	4.0521	0.0041
		5	4.05204	0.0027
		6	4.052	0.0017
		7	4.05198	0.0012
1	4.6488128272	1	4.67824	0.6330
		2	4.65145	0.0567
		3	4.64956	0.0161
		4	4.6492	0.0083
		5	4.64907	0.0055
		6	4.64899	0.0038
		7	4.64893	0.0025
2	5.4757846463	1	5.51987	0.8051
		2	5.48037	0.0837
		3	5.47715	0.0249
		4	5.47651	0.0132
		5	5.47626	0.0087
		6	5.47612	0.0061
		7	5.47602	0.0043
5	7.0134792987	1	7.08229	0.9811
		2	7.02152	0.1146
		3	7.01598	0.0357
		4	7.01482	0.0191
		5	7.01437	0.0127
		6	7.01412	0.0091
		7	7.01394	0.0066
20	10.6432159591	1	10.7643	1.1377
		2	10.6586	0.1445
		3	10.6482	0.0468
		4	10.6459	0.0252
		5	10.645	0.0168
		6	10.6445	0.0121
		7	10.6442	0.0092

Table 5.4: First excited state energies, percent differences, and calculation times for the anharmonic oscillator using the harmonic oscillator first excited state Eq. 4.2 in CMX-LT.

λ	Martin, Castro, and Paz	Order	CMX-LT		
			Energy	% difference	Time (s)
2	5.4757846463	1	5.51987	0.8051	0.4 ± 0.1
		2	5.48037	0.0837	8.9 ± 0.5
		3	5.47715	0.0249	15.1 ± 1.3
		4	5.47651	0.0132	25.4 ± 1.7
		5	5.47626	0.0087	30.8 ± 2.4
		6	5.47612	0.0061	37.3 ± 6.1
		7	5.47602	0.0043	29.7 ± 0.3

Table 5.5: Ground state energies and percent differences for the anharmonic oscillator using the hyperbolic secant function, Eq. 4.9, in CMX-LT.

λ	Martin, Castro, and Paz	Order	CMX-LT	
			Energy	% difference
0.5	1.2418540431	1	1.38901	11.850
		2	1.33341	7.373
		3	1.31711	6.060
		4	1.30956	5.452
		5	1.30524	5.104
1	1.3923515801	1	1.58809	14.058
		2	1.52277	9.367
		3	1.5027	7.925
		4	1.49318	7.242
		5	1.48767	6.846
2	1.6075413481	1	1.86551	16.047
		2	1.78638	11.125
		3	1.76148	9.576
		4	1.74952	8.832
		5	1.74253	8.397
5	2.0183406575	1	2.38345	18.090
		2	2.27891	12.910
		3	2.24547	11.253
		4	2.22927	10.451
		5	2.21976	9.979
20	3.0099449478	1	3.6097	19.926
		2	3.44651	14.504
		3	3.39378	12.752
		4	3.36809	11.899
		5	3.35296	11.396

Table 5.6: Ground state energies and percent differences for the anharmonic oscillator using the cosine function, Eq. 4.10, in CMX-LT.

λ	Martin, Castro, and Paz	Order	CMX-LT	
			Energy	% difference
0.5	1.2418540431	1	1.26076	1.522
		2	1.23735	-0.363
		3	1.24519	0.269
		4	1.24033	-0.123
		5	1.25452	1.020
1	1.3923515801	1	1.41068	1.316
		2	1.38807	-0.308
		3	1.39571	0.241
		4	1.3908	-0.111
		5	1.40409	0.843
2	1.6075413481	1	1.62633	1.169
		2	1.60305	-0.279
		3	1.61097	0.213
		4	1.6056	-0.121
		5	1.61932	0.733
5	2.0183406575	1	2.04	1.073
		2	2.013	-0.265
		3	2.02207	0.185
		4	2.01644	-0.094
		5	2.03152	0.653
20	3.0099449478	1	3.03907	0.968
		2	3.00223	-0.256
		3	3.01482	0.162
		4	3.01027	0.011
		5	3.02831	0.610

Table 5.7: Ground state energies, percent differences, and calculation times for the anharmonic oscillator using the cosine function Eq. 4.10 in CMX-LT.

λ	Martin, Castro, and Paz	Order	CMX-LT		
			Energy	% difference	Time (s)
2	1.6075413481	1	1.62633	1.169	2.70 ± 0.32
		2	1.60305	-0.279	14.0 ± 1.7
		3	1.61097	0.213	40.3 ± 1.2
		4	1.6056	-0.121	84.9 ± 3.7
		5	1.61932	0.733	123.8 ± 3.6

5.1.3 Lanczos Tri-Diagonalization

Lanczos tri-diagonalization is the fastest of the methods by a large margin. It also generates approximations to multiple energy states at the same time, however most of those approximations are extremely poor, with the second excited state energies being actually worse than the best ones obtained with CMX, and the first excited state energies being less accurate still. However, the ground state energies are as good as the CMX-LT results. Results for the ground and first excited states with this method can be found in Table 5.8.

Table 5.8: Ground state and first excited state energies, percent differences, and calculation times for the anharmonic oscillator using the harmonic oscillator ground state, Eq. 4.2, with Lanczos Tri-Diagonalization.

λ	Martin, Castro, and Paz	Order	Lanczos Energy	Ground State % difference	Time (s)	Excited State Energy	Excited State % difference
0.5	Ground:	2	1.24239	0.0432		17.097	321.947
	1.2418540431	3	1.24201	0.0126		15.4682	281.749
	1st Excited:	4	1.24194	0.0069		14.8309	266.020
	4.0519323386	5	1.24191	0.0045		14.3219	253.459
		6	1.24189	0.0029		13.6556	237.015
		7	1.24188	0.0021		12.6078	211.155
1	Ground:	2	1.39363	0.0918		21.2276	356.624
	1.3923515801	3	1.39277	0.0301		18.7216	302.718
	1st Excited:	4	1.39258	0.0164		17.7542	281.908
	4.6488128272	5	1.39251	0.0114		17.0787	267.378
		6	1.39247	0.0085		16.3784	252.314
		7	1.39244	0.0064		15.4822	233.036
2	Ground:	2	1.61001	0.154	14.1 ± 1.0	26.64	386.506
	1.6075413481	3	1.6084	0.053	28.1 ± 0.2	23.0381	320.727
	1st Excited:	4	1.60802	0.030	29.8 ± 1.9	21.6546	295.461
	5.4757846463	5	1.60788	0.021	46.3 ± 9.3	20.7514	278.967
		6	1.60779	0.0155	36.0 ± 1.2	19.9202	263.787
		7	1.60774	0.0124	51.3 ± 1.4	18.9854	246.716
5	Ground:	2	2.02305	0.233		36.1819	415.891
	2.0183406575	3	2.02009	0.087		28.6661	338.414
	1st Excited:	4	2.01934	0.050		28.6661	308.729
	7.0134792987	5	2.01904	0.035		27.3647	290.173
		6	2.01888	0.0267		26.2581	274.395
		7	2.01876	0.0208		25.1221	258.197
20	Ground:	2	3.01953	0.318		57.6055	441.241
	3.0099449478	3	3.01368	0.124		48.2848	353.667
	1st Excited:	4	3.01212	0.072		44.7172	320.147
	10.6432159591	5	3.01148	0.051		42.5464	299.751
		6	3.01113	0.0394		40.7895	283.244
		7	3.01089	0.0314		39.0898	267.274

Chapter 6

Conclusions

In almost all of these cases these simple methods were able to produce results accurate to 2 or 3 significant figures with quite limited computational effort. The exceptions were the energies generated with the hyperbolic secant-based wave function, the energy of the second excited state and all excited states generated by the Lanczos tri-diagonalization method. It is likely that the trial wave functions in these cases were simply too different from the true ones for the approximation to converge rapidly, and so much higher order calculations would have been required. Varying the kurtosis of the trial wave function proved unwise in general, with both options generating much worse results than those given by the Gaussian function which was expected to be the best match to the true wave function. More study could be valuable here, examining a potential for which a higher or lower kurtosis function would be expected to verify that the Gaussian is not simply the best trial wave function choice in all cases, but rather that the best choice is a function which is likely to be similar to the true wave function.

Overall, the CMX-HW and CMX-LT had nearly identical calculation times, but the CMX-LT appears to correct by more with each order, which gives it better results in most cases, the exception being the cosine-based wave function, for which it results in larger

oscillations. Since all necessary figures to instantaneously process a lower order approximation will be stored in memory until the program is closed, it will likely be beneficial to check some of those for such oscillations. Lanczos Tri-Diagonalization was clearly the best of the methods, however: it matches the accuracy of CMX-LT and computes more rapidly. Preconditioning with Variational Analysis was also shown to be extremely valuable, improving the accuracy of the approximation by multiple orders of magnitude in the percent difference and generating a smallest error of just 0.0012%, and so this should certainly be used whenever possible.

Future work could take several directions. One is simply to apply these same techniques to other potentials, which we did not have time to do in this project. Another interesting avenue would be to try to optimize the parameter for other terms, particularly I_2 , which is the variance of the energy, and should therefore go to zero if the wave function is exact. There are also inconsistencies in the computation time, both for the 6th and 7th order of the first excited state, as well as significant variation with λ , and it would be instructive to investigate these and try to determine a cause.

Bibliography

- [1] D. J. Griffiths, *Introduction to Quantum Mechanics* (Pearson Education, London, 2005).
- [2] P. Martin, E. Castro, J. L. Paz. *Rev. Mex. Fis.* **58**, 301 (2012).
- [3] N. S. Witte. *Int. J. Mod. Phys. B* **11**, 1503 (1997).
- [4] S. Koonin, D. Meredith. *Computational Physics: Fortran Version* (Addison-Wesley Publishing Company, Reading, 1990).
- [5] D. Horn and M. Weinstein. *Phys. Rev. D.* **30**, 1256 (1984).
- [6] J. Cioslowski. *Phys. Rev. Lett.* **58**, 83 (1987).
- [7] J. Mancini, R. Murawski, V. Fessatidis, and S. Bowen. *Phys. Rev. B* **72**, 214405 (2005).
- [8] P. Knowles, *Chem. Phys. Lett.* 134, 512 (1987).
- [9] Kesheng Wu, Horst Simon, L. W. Wang. *J. Comput. Phys.* **154**, 156 1999.
- [10] S. Dawson. *AIP Conf. Proc.* 1116: 11-34, 2009.
- [11] J. Taylor, C. Zafiratos, M. Dubson. *Modern Physics for Scientists and Engineers* (Pearson Education, Upper Saddle River, 2004).

[12] A. C. Aitken. *Statistical Mathematics* (Oliver and Boyd, Edinburgh, 1939).

Appendix A

CMX Code

```
\[Psi]1[x_, a_] := ((a/Pi)^0.25) Exp[-(a*(x^2))/2]
Integrate[\[Psi]1[x, a]*\[Psi]1[x, a],
{x, -\[Infinity], \[Infinity]}]

\[Psi]0[x_, a_] := ((a/Pi)^0.25) Exp[-(a*(x^2))/2]
V0[x_] := x^2 + (b)*x^4
EE[a_] :=
Integrate[\[Psi]0[x,
a]*(-1) Laplacian[\[Psi]0[x,
a], {x}], {x, -\[Infinity], \[Infinity]}]
FF[a_] :=
Integrate[\[Psi]0[x, a]*
V0[x]*\[Psi]0[x, a], {x, -\[Infinity], \[Infinity]}]
EE[a] + FF[a]

D[0.499999999999999994 a^1. + (0.5 a + 0.75 b)/a^2., a]
```

Solve[$a^3 - a - 3 b == 0$, a]

aa[b_] := (2/3)^(1/3)/

(27 b + **Sqrt**[3] **Sqrt**[-4 + 243 b^2])^(1/3)

+ (27 b + **Sqrt**[3] **Sqrt**[-4 + 243 b^2])^(1/3)/

(2^(1/3) 3^(2/3))

bb =;

\[Psi][x_] := ((aa[bb]/**Pi**)^(0.25)) **Exp**[-(aa[bb]*(x^2))/2]

V[x_] := x^2 + (bb)*x^4

H[f_] := **Simplify**[((-1) **Laplacian**[f, {x}] + V[x] f)]

AA[n_] :=

Integrate[\[Psi][x]*

Nest[H, \[Psi][x], n], {x, -\[Infinity], \[Infinity]}]

J[1] := J[1] =

Integrate[\[Psi][x]*H[\[Psi][x]],

{x, -\[Infinity], \[Infinity]}]

J[n_] := J[n] =

AA[n] - **Sum**[(**Binomial**[n - 1, k])*(J[k + 1])*AA[n - k - 1],

{k, 0, n - 2}]

S[1, n_] := S[1, n] = J[n]

S[m_, n_] :=

S[m, n] = (S[m - 1, n]*S[m - 1, n + 2])

$$- (S[m - 1, n + 1])^2$$

HW[n_] :=

$$J[1] - \text{Sum}[\left(\frac{(S[m, 2])^2}{\text{Product}[(S[k, 3]), \{k, 1, m\}]}\right), \{m, 1, n - 1\}]$$

LT[n_] :=

$$J[1] - \text{Det}[(\text{MatrixForm}[\text{Table}[J[j], \{i, 1\}, \{j, 2, n\}]]).$$

(Inverse[MatrixForm[

$$\text{Table}[J[1 + i + j], \{i, n - 1\}, \{j, n - 1\}]]]).$$

(MatrixForm[Table[J[i], \{i, 2, n\}, \{j, 1\}]]])]

Appendix B

Lanczos Tri-Diagonalization Code

```
\[Beta][1] = 0;
v[0] = 0;
v[1] := ((aa[bb]/Pi)^(0.25)) Exp[-(aa[bb]*(x^2))/2]
w[j_] := H[v[j]]
u[j_] := w[j] - \[Alpha][j]*v[j] - \[Beta][j]*v[j - 1]
\[Beta][j_] := \[Beta][j] = (Integrate[u[j - 1]*u[j - 1],
  {x, -\[Infinity], \[Infinity]}])^0.5
\[Alpha][j_] := \[Alpha][j] = (Integrate[w[j]*v[j],
  {x, -\[Infinity], \[Infinity]}])
v[j_] := u[j - 1]/\[Beta][j]

T[n_] := MatrixForm[
  Table[Piecewise[{{\[Alpha][i], j - i == 0},
    {\[Beta][i], i - j == 1}, {\[Beta][j], j - i == 1}}, 0],
    {i, n}, {j, n}]]
```

Appendix C

Further Data Tables

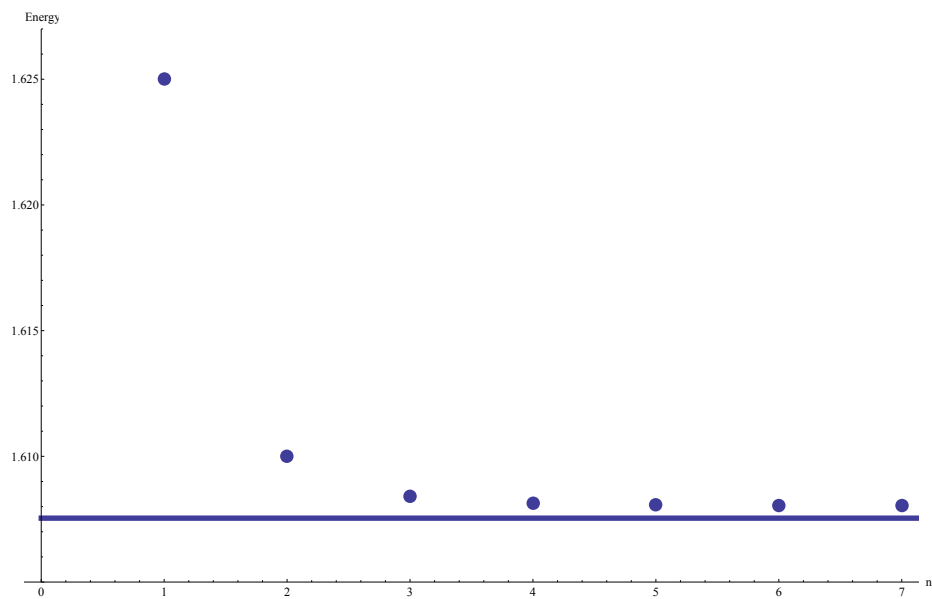


Figure C.1: Graph of energy approximation vs. order for CMX-HW, with comparison to the Martin, Castro, and Paz result, for $\lambda = 2$.

Table C.1: Ground state energies and percent differences for the anharmonic oscillator using the harmonic oscillator ground state Eq. 4.2 in CMX-HW.

λ	Martin, Castro, and Paz	Order	CMX-HW Energy	% difference
0.5	1.24185404314	1	1.24803	0.4973
		2	1.24239	0.0432
		3	1.24201	0.0126
		4	1.24195	0.0077
		5	1.24194	0.0069
		6	1.24193	0.0061
		7	1.24193	0.0061
1	1.3923515801	1	1.40332	0.7878
		2	1.39363	0.0918
		3	1.39276	0.0293
		4	1.39262	0.0193
		5	1.39259	0.0171
		6	1.39258	0.0164
		7	1.39258	0.0164
2	1.6075413481	1	1.625	1.0860
		2	1.61	0.1529
		3	1.6084	0.0534
		4	1.60813	0.0366
		5	1.60806	0.0323
		6	1.60805	0.0316
		7	1.60805	0.0316
5	2.0183406575	1	2.04704	1.4219
		2	2.02303	0.2323
		3	2.02009	0.0867
		4	2.01956	0.0604
		5	2.01944	0.0545
		6	2.01942	0.0535
		7	2.01942	0.0535
20	3.0099449478	1	3.0625	1.746
		2	3.0195	0.3174
		3	3.01367	0.1238
		4	3.01261	0.0885
		5	3.01236	0.0802
		6	3.01233	0.0792
		7	3.01233	0.0792

Table C.2: Ground state energies, percent differences, and calculation times for the anharmonic oscillator using Eq. 4.2 in CMX-HW.

λ	Martin, Castro, and Paz	Order	CMX-HW Energy	% difference	Time (s)
2	1.6075413481	1	1.625	1.0860	5.7 ± 0.4
		2	1.61	0.1529	11.5 ± 1.6
		3	1.6084	0.0534	20.2 ± 3.7
		4	1.60813	0.0366	29.2 ± 0.7
		5	1.60806	0.0323	53.4 ± 2.0
		6	1.60805	0.0316	72.0 ± 7.1
		7	1.60805	0.0316	79.7 ± 1.4

Table C.3: First excited state energies, percent differences, and calculation times for the anharmonic oscillator using the harmonic oscillator first excited state Eq. 4.3 in CMX-HW.

λ	Martin, Castro, and Paz	Order	CMX-HW	
			Energy	% difference
0.5	4.0519323386	1	4.06992	0.4439
		2	4.05321	0.0315
		3	4.05227	0.0083
		4	4.05213	0.0049
		5	4.0521	0.0041
		6	4.05209	0.0039
		7	4.05209	0.0039
1	4.6488128272	1	4.67824	0.6330
		2	4.65145	0.0567
		3	4.64956	0.0161
		4	4.64928	0.0100
		5	4.6492	0.0083
		6	4.64919	0.0081
		7	4.64919	0.0081
2	5.4757846463	1	5.51987	0.8051
		2	5.48037	0.0837
		3	5.47715	0.0249
		4	5.47666	0.0160
		5	5.47652	0.0134
		6	5.4765	0.0131
		7	5.4765	0.0131
5	7.0134792987	1	7.08229	0.9811
		2	7.02152	0.1146
		3	7.01598	0.0357
		4	7.01511	0.0233
		5	7.01487	0.0198
		6	7.01484	0.0194
		7	7.01484	0.0194
20	10.6432159591	1	10.7643	1.1377
		2	10.6586	0.1445
		3	10.6482	0.0468
		4	10.6465	0.0309
		5	10.646	0.0262
		6	10.646	0.0262
		7	10.646	0.0262

Table C.4: First excited state energies, percent differences, and calculation times for the anharmonic oscillator using the harmonic oscillator first excited state Eq. 4.3 in CMX-HW.

λ	Martin, Castro, and Paz	Order	CMX-HW		
			Energy	% difference	Time (s)
2	5.4757846463	1	5.51987	0.8051	0.671 ± 0.063
		2	5.48037	0.0837	8.15 ± 0.77
		3	5.47715	0.0249	9.58 ± 0.73
		4	5.47666	0.0160	25.7 ± 3.3
		5	5.47652	0.0134	33.2 ± 6.4
		6	5.4765	0.0131	43.6 ± 9.2
		7	5.4765	0.0131	29.9 ± 0.3

Table C.5: Second excited state energies and percent differences for the anharmonic oscillator using the harmonic oscillator second excited state Eq. 4.4 in CMX-HW.

λ	Martin, Castro, and Paz	Order	CMX-HW Energy	% difference
0.5	7.3969068694	1	92.9042	1155.987
		2	48.4152	554.533
		3	33.6271	354.610
		4	28.1057	279.966
		5	26.29	255.419
		6	25.9148	250.346
		7	25.8865	249.964
1	8.6550499823	1	108.662	1155.475
		2	56.6446	554.469
		3	39.3579	354.739
		4	32.9065	280.200
		5	30.7861	255.701
		6	30.3481	250.640
		7	30.3151	250.259
2	10.3585833647	1	129.996	1154.959
		2	67.7847	554.382
		3	47.1146	354.836
		4	39.4036	280.396
		5	36.8705	255.942
		6	36.3475	250.893
		7	36.3081	250.512
5	13.4677303948	1	168.939	1154.398
		2	88.1158	554.274
		3	61.2674	354.920
		4	51.2558	280.582
		5	47.9689	256.177
		6	47.2906	251.140
		7	47.2395	250.761
20	20.6941109272	1	259.481	1153.888
		2	135.373	554.162
		3	94.1549	354.984
		4	78.7908	280.740
		5	73.7492	256.378
		6	72.7093	251.353
		7	72.6311	250.975

Table C.6: Second excited state energies, percent differences, and calculation times for the anharmonic oscillator using the harmonic oscillator second excited state, Eq. 4.4, in CMX-HW.

λ	Martin, Castro, and Paz	Order	CMX-HW		
			Energy	% difference	Time (s)
		2	67.7847	554.382	8.3 ± 1.0
		3	47.1146	354.836	12.5 ± 1.6
		4	39.4036	280.396	22.1 ± 3.1
		5	36.8705	255.942	31.9 ± 4.2
		6	36.3475	250.893	20.8 ± 0.1
		7	36.3081	250.512	28.4 ± 1.0

Table C.7: Second excited state energies and percent differences for the anharmonic oscillator using the harmonic oscillator second excited state, Eq. 4.4, in CMX-LT.

λ	Martin, Castro, and Paz	Order	CMX-LT	
			Energy	% difference
0.5	7.3969068694	1	92.9042	1155.987
		2	48.4152	554.533
		3	33.6271	354.610
		4	26.2652	255.084
		5	21.8748	195.729
		6	18.9712	156.475
		7	16.9182	128.720
1	8.6550499823	1	108.662	1155.475
		2	56.6446	554.469
		3	39.3579	354.739
		4	30.7559	255.352
		5	25.6296	196.123
		6	22.2432	156.997
		7	19.8529	129.379
2	10.3585833647	1	129.996	1154.959
		2	67.7847	554.382
		3	47.1146	354.836
		4	36.833	255.580
		5	30.7101	196.470
		6	26.6697	157.465
		7	23.8228	129.981
5	13.4677303948	1	168.939	1154.398
		2	88.1158	554.274
		3	61.2674	354.920
		4	47.9183	255.801
		5	39.9744	196.816
		6	34.7388	157.941
		7	31.0567	130.601
20	20.6941109272	1	259.481	1153.888
		2	135.373	554.162
		3	94.1549	354.984
		4	73.6689	255.990
		5	61.4862	197.119
		6	53.4658	158.362
		7	47.8356	131.156

Table C.8: Second excited state energies, percent differences, and calculation times for the anharmonic oscillator using the harmonic oscillator second excited state, Eq. 4.4, in CMX-LT.

λ	Martin, Castro, and Paz	Order	CMX-LT		
			Energy	% difference	Time (s)
2	10.3585833647	1	129.996	1154.959	3.61 ± 0.35
		2	67.7847	554.382	8.45 ± 0.58
		3	47.1146	354.836	11.7 ± 1.1
		4	36.833	255.580	16.3 ± 3.0
		5	30.7101	196.470	18.1 ± 0.3
		6	26.6697	157.465	20.8 ± 0.1
		7	23.8228	129.981	28.4 ± 0.8

Table C.9: Ground state energies, percent differences, and calculation times for the anharmonic oscillator using the hyperbolic secant function, Eq. 4.9, in CMX-HW.

λ	Martin, Castro, and Paz	Order	CMX-HW	
			Energy	% difference
0.5	1.2418540431	1	1.38901	11.850
		2	1.33341	7.373
		3	1.31711	6.060
		4	1.31437	5.839
		5	1.31422	5.827
1	1.3923515801	1	1.58809	14.058
		2	1.52277	9.367
		3	1.5027	7.925
		4	1.49919	7.673
		5	1.49899	7.659
2	1.6075413481	1	1.86551	16.047
		2	1.78638	11.125
		3	1.76148	9.576
		4	1.75702	9.299
		5	1.75676	9.282
5	2.0183406575	1	2.38345	18.090
		2	2.27891	12.910
		3	2.24547	11.253
		4	2.23939	10.952
		5	2.23903	10.934
20	3.0099449478	1	3.6097	19.926
		2	3.44651	14.504
		3	3.39378	12.752
		4	3.38408	12.430
		5	3.3835	12.410

Table C.10: Ground state energies and percent differences for the anharmonic oscillator using the cosine wave function, Eq. 4.10, in CMX-HW.

λ	Martin, Castro, and Paz	Order	CMX-HW	
			Energy	% difference
0.5	1.2418540431	1	1.26076	1.522
		2	1.23735	-0.363
		3	1.24519	0.269
		4	1.24523	0.272
		5	1.24508	0.260
1	1.3923515801	1	1.41068	1.316
		2	1.38807	-0.308
		3	1.39571	0.241
		4	1.39575	0.244
		5	1.39563	0.235
2	1.6075413481	1	1.62633	1.169
		2	1.60305	-0.279
		3	1.61097	0.213
		4	1.61102	0.216
		5	1.61094	0.211
5	2.0183406575	1	2.04	1.073
		2	2.013	-0.265
		3	2.02207	0.185
		4	2.02215	0.189
		5	2.02206	0.184
20	3.0099449478	1	3.03907	0.968
		2	3.00223	-0.256
		3	3.01482	0.162
		4	3.01489	0.164
		5	3.01464	0.156

Table C.11: Ground state energies, percent differences, and calculation times for the anharmonic oscillator using the cosine wave function, Eq. 4.10, in CMX-HW.

λ	Martin, Castro, and Paz	Order	CMX-HW		
			Energy	% difference	Time (s)
2	1.6075413481	1	1.62633	1.169	2.00 ± 0.35
		2	1.60305	-0.279	12.11 ± 0.56
		3	1.61097	0.213	33.56 ± 0.13
		4	1.61102	0.216	68.4 ± 2.6
		5	1.61094	0.211	110.6 ± 8.8